Arab J Sci Eng (2014) 39:5085–5093
DOI 10.1007/s13369-014-1016-8

RESEARCH ARTICLE - MECHANICAL ENGINEERING

Flow of Micropolar Fluid Between Parallel Plates with Soret and Dufour Effects

D. Srinivasacharya · Mekonnen Shiferaw

Received: 7 October 2012 / Accepted: 31 March 2013 / Published online: 23 April 2014

Abstract The flow of a steady, incompressible, micropolar fluid between parallel plates is studied in the presence of cross-diffusion effects. The governing non-linear systems of differential equations are solved by the homotopy analysis method. The non-dimensional velocity, temperature and concentration profiles are displayed graphically for different values of Dufour number, Soret number and coupling number. In addition, the skin-friction coefficient, heat and mass transfer rates are shown in a tabular form.

Keywords Mixed convection · Micropolar fluid · Soret and Dufour effects · Heat and mass transfer

الخلاصة

تمت دراسة سائل مطرد، غير منضغط ومتناهي الصغر في القطبية بين لوحات موازية في وجود آثار انتشار متقاطع. وحُلّت الأنظمة غير الخطية الحاكمة للمعادلات التفاضلية باستخدام أسلوب التحليل هوموتوبي (HAM)، وعُرضت السرعة غير البعدية، وملامح درجة الحرارة والتركيز بيانيا لقيم مختلفة من عدد دوفور، وعدد سورت وعددالاقتران. بالإضافة إلى ذلك، تم عرض معامل احتكاك الجلد ومعدلات انتقال الحرارة والكتلة في شكل جداول.

D. Srinivasacharya (✉)
Department of Mathematics, National Institute of Technology, Warangal 506004, Andhra Pradesh, India
e-mail: dsc@nitw.ac.in; dsrinivasacharya@yahoo.com

M. Shiferaw
Department of Mathematics, Arba Minch University, Arba Minch, Ethiopia

1 Introduction

It is well known that most fluids which are encountered in chemical and allied processing applications do not satisfy the classical Newton's law and are accordingly known as non-Newtonian fluids. Due to the important applications of non-Newtonian fluids in biology, physiology, technology, and industry, considerable efforts have been directed towards the analysis and understanding of such fluids. The prediction of heat or mass transfer characteristics of non-Newtonian fluids is very important because of its practical engineering applications, such as thermal design of industrial equipment dealing with molten plastics, polymeric liquids, foodstuffs, or slurries, etc. A number of mathematical models have been proposed to explain the rheological behavior of non-Newtonian fluids. Also, there exist several approaches to study the mechanics of fluids with a substructure. Ericson [1,2] derived field equations which account for the presence of substructures in the fluid. It has been experimentally demonstrated by Hoyt and Fabula [3] that fluids containing a small amount of polymeric additives display a reduction in skin friction. The fluid model introduced by Eringen [4] exhibits some microscopic effects arising from the local structure and micromotion of fluid elements. Further, they sustain couple stresses and include classical Newtonian fluid as a special case. The model of micropolar fluid represents fluids consisting of rigid, randomly oriented (or spherical) particles suspended in a viscous medium where the deformation of the particles is ignored. Physically, micropolar fluids may be described as non-Newtonian fluids consisting of dumb-bell molecules or short rigid cylindrical element, polymer fluids, fluid suspension, etc. Micropolar fluids have been shown to accurately simulate the flow characteristics of polymeric additives, geomorphological sediments, colloidal suspensions, haematological suspensions, liquid crystals, lubricants etc.

The presence of dust or smoke, particularly in a gas, may also be modeled using micropolar fluid dynamics. The mathematical theory of equations of micropolar fluids and applications of these fluids in the theory of lubrication and porous media are presented by Lukaszewicz [5]. The heat and mass transfer in micropolar fluids is important in the context of chemical engineering, aerospace engineering and industrial manufacturing processes.

When heat and mass transfer occur simultaneously in a moving fluid, the relations between the flux and the driving potentials are of a more intricate nature. It has been observed that an energy flux can be generated not only by temperature gradients but also by concentration gradients. The energy flux caused by a concentration gradient is termed the diffusion-thermo (Dufour) effect. On the other hand, mass flux can also be created by temperature gradients and this embodies the thermal-diffusion (Soret) effect. In most of the studies related to heat and mass transfer process, Soret and Dufour effects are neglected on the basis that they are of a smaller order of magnitude than the effects described by Fouriers and Ficks laws. But these effects are considered as second order phenomena and may become significant in areas such as hydrology, petrology, geosciences, etc. The Soret effect, for instance, has been utilized for isotope separation and in mixture between gases with very light molecular weight and of medium molecular weight. The Dufour effect was recently found to be of order of considerable magnitude so that it cannot be neglected [6]. Dursunkaya and Worek [7] studied diffusion-thermo and thermal-diffusion effects in transient and steady natural convection from a vertical surface, whereas Kafoussias and Williams [8] presented the same effects on mixed convective and mass transfer steady laminar boundary layer flow over a vertical flat plate with temperature dependent viscosity. Awad and Sibanda [9] studied the Dufour and Soret effects on heat and mass transfer in a micropolar fluid in a horizontal channel. Free convection heat and mass transfer flow in a vertical channel with the Dufour effect was studied by Ajibade and Jha [10]. Olanrewaju and Makinde [11] analyzed the free convective heat and mass transfer of an incompressible, electrically conducting fluid past a moving vertical plate in the presence of suction and injection with thermal diffusion (Soret) and diffusion-thermo (Dufour) effects. Srinivasacharya and Kaladhar [12] presented the natural convection heat and mass transfer of a couple stress fluid in an annulus with Soret and Dufour effects. Elaiw et al. [13] studied the effect of variable viscosity on the vortex instability of horizontal mixed convection boundary layer flow in a saturated porous medium with variable wall temperature. Mokheimer [14] numerically investigated the entropy generation due to laminar mixed convection in the entrance of vertical channel between two isothermal/adiabatic parallel plates.

In the present paper, we analyze the effect of Soret and Dufour on steady mixed convective micropolar fluid flow between parallel plates. The governing non-linear differential equations have been solved by using the homotopy analysis method (HAM). It was first proposed by Liao [15] in 1992 and is considered as one of the most efficient methods in solving different types of non-linear equations such as coupled, decoupled, homogeneous and non-homogeneous. Also, HAM provides us great freedom to choose different base functions to express solutions of a non-linear problem [16]. The convergent region of the HAM solution for the model is introduced graphically and examined. The velocity, microrotation, temperature, and concentration functions are shown graphically for various parameters.

2 Mathematical Formulation

Consider a steady, laminar, mixed convection flow of incompressible micropolar fluid between two parallel plates distance h apart. Choose the coordinate system such that the origin is on the lower plate, x-axis is along the flow direction and y-axis is perpendicular to the plates. The lower plate $y = 0$ is maintained at a constant temperature T_1 and concentration C_1, while the upper plate $y = h$ at a constant temperature T_2 and concentration C_2. Since the boundaries in the x direction are of infinite dimensions, without loss of generality, we assume that the physical quantities depend on y only. The fluid properties are assumed to be constant except for density variations in the buoyancy force term. In addition, the Soret and Dufour effects are considered. The flow is a mixed convection caused by buoyancy forces and uniform pressure gradient in the direction of x. The fluid velocity vector $\bar{q} = (u; v)$ is assumed to be parallel to the x-axis, so that only the x component u of the velocity vector does not vanish but the transpiration cross-flow velocity v_0 remains constant, where $v_0 < 0$ is the velocity of suction and $v_0 > 0$ is the velocity of injection.

With the above assumptions and Boussinesq approximations with energy and concentration, the equations governing the flow of an incompressible micropolar fluid are:

$$v = v_0 = \text{constant} \tag{1}$$

$$(\mu + \kappa)\frac{\partial^2 u}{\partial y^2} - \rho v_0 \frac{\partial u}{\partial y} + \rho g\{\beta_T(T - T_1) + \beta_c(C - C_1)\} - \frac{\partial P}{\partial x} + \kappa \frac{\partial \Gamma}{\partial y} = 0 \tag{2}$$

$$\gamma \frac{\partial^2 \Gamma}{\partial y^2} - \rho j v_0 \frac{\partial \Gamma}{\partial y} - 2\kappa\Gamma - \kappa \frac{\partial u}{\partial y} = 0 \tag{3}$$

$$k_f \frac{\partial^2 T}{\partial y^2} - c_p \rho v_0 \frac{\partial T}{\partial y} + (\mu + \kappa)\left(\frac{\partial u}{\partial y}\right)^2$$

$$+\gamma\left(\frac{\partial \Gamma}{\partial y}\right)^2+2\kappa\left(\Gamma^2+\Gamma\frac{\partial u}{\partial y}\right)+\frac{DK_{\mathrm{T}}}{C_{\mathrm{s}}}\frac{\partial^2 C}{\partial y^2}=0 \quad (4)$$

$$D\frac{\partial^2 C}{\partial y^2}-v_0\frac{\partial C}{\partial y}+\frac{DK_{\mathrm{T}}}{T_{\mathrm{m}}}\frac{\partial^2 T}{\partial y^2}=0 \quad (5)$$

where u is velocity components in the x directions Γ is microrotation, ρ and j are the fluid density and gyration parameter, μ, κ and γ are the material constants (viscosity coefficients), g is the acceleration due to gravity, p is pressure, β_{T} is the coefficient of thermal expansion, β_c is the coefficient of solutal expansion, k_{f} the coefficient of thermal conductivity, D is the mass diffusivity, c_{p} is the specific heat of fluid, C_{s} is the concentration susceptibility, T_{m} is the mean fluid temperature, and K_{T} is the thermal diffusion ratio.

The boundary conditions are:

$$u=0,\quad v=v_0,\quad \Gamma=0,\quad T=T_1,\quad C=C_1,\quad \text{at}\quad y=0 \quad (6a)$$

$$u=0,\quad v=v_0,\quad \Gamma=0,\quad T=T_2,\quad C=C_2,\quad \text{at}\quad y=h \quad (6b)$$

Introducing the following non-dimensional variables:

$$\eta=\frac{y}{h},\quad u=U_0 f(\eta),\quad \Gamma=\frac{U_0}{h}\omega(\eta),$$
$$\theta(\eta)=\frac{T-T_1}{T_2-T_1},\quad \phi(\eta)=\frac{C-C_1}{C_2-C_1} \quad (7)$$

in Eqs. (1)–(5), we get the following non-linear system of differential equations

$$\frac{1}{1-N}f''-Rf'+\frac{N}{1-N}\omega'+\frac{Gr_{\mathrm{T}}}{Re}\theta+\frac{Gr_{\mathrm{c}}}{Re}\phi-A=0 \quad (8)$$

$$\frac{2-N}{m_{\mathrm{p}}^2}\omega''-a_j\frac{1-N}{N}R\omega'-(2\omega+f')=0 \quad (9)$$

$$\theta''-RPr\theta'+\frac{Br}{1-N}\left[f'^2+\frac{N(2-N)}{m_{\mathrm{p}}^2}\omega'^2+2N(\omega^2-\omega f')\right]+D_{\mathrm{f}}Pr\phi''=0 \quad (10)$$

$$\frac{1}{Sc}\phi''-R\phi'+S_{\mathrm{r}}\theta''=0 \quad (11)$$

where primes denote differentiation with respect to η, $Sc=\frac{\nu}{D}$ is the Schmidt number, $Pr=\frac{\mu c_{\mathrm{p}}}{k_{\mathrm{f}}}$ is the Prandtl number, $Re=\frac{\rho U_0 h}{\mu}$ is the Reynolds number, $S_{\mathrm{r}}=\frac{DK_{\mathrm{T}}(T_2-T_1)}{\nu T_{\mathrm{m}}(C_2-C_1)}$ is the Soret number, $D_{\mathrm{f}}=\frac{DK_{\mathrm{T}}(C_2-C_1)}{\nu c_{\mathrm{s}}C_{\mathrm{p}}(T_2-T_1)}$ is the Dufour number, $R=\frac{\rho v_0 h}{\mu}$ is the suction/injuction parameter, $N=\frac{\kappa}{\mu+\kappa}$ is coupling number, $Gr_{\mathrm{T}}=\frac{g\rho^2\beta_T(T_2-T_1)h^3}{\mu^2}$ is temperature Grashof number, $Gr_{\mathrm{c}}=\frac{g\rho^2\beta_c(C_2-C_1)h^3}{\mu^2}$ is the mass Grashof number, $A=\frac{h^2}{\mu U_0}\frac{\mathrm{d}P}{\mathrm{d}x}$ is the constant pressure gradient, $m_{\mathrm{p}}^2=\frac{h^2\kappa(2\mu+\kappa)}{\gamma(\mu+\kappa)}$ is the micropolar parameter, $a_j=\frac{j}{h^2}$ is the micro-inertial density parameter, $Br=\frac{\mu U_0^2}{k_{\mathrm{f}}(T_2-T_1)}$ is the Brinkman number.

Boundary conditions (6) in terms of f, ω, θ and ϕ become

$$f=0,\quad \omega=0,\quad \theta=0,\quad \phi=0\quad \text{at}\quad \eta=0 \quad (12a)$$

$$f=0,\quad \omega=0,\quad \theta=1,\quad \phi=1\quad \text{as}\quad \eta=1 \quad (12b)$$

3 The HAM Series Solution

For HAM solutions, we choose the initial approximations of $f(\eta), \omega(\eta), \theta(\eta)$ and $\phi(\eta)$ as follows:

$$f_0(\eta)=0,\quad \omega_0(\eta)=0,\quad \theta_0(\eta)=\eta,\quad \phi_0(\eta)=\eta \quad (13)$$

and choose the auxiliary linear operators $L=\frac{\partial^2}{\partial\eta^2}$ such that $L(c_1+c_2\eta)=0$ where c_1 and c_2 are constants. Introducing non-zero auxiliary parameters h_1, h_2, h_3 and h_4, we develop the zeroth-order deformation as follows:

$$(1-p)L[f(\eta;p)-f_0(\eta)]=ph_1N_1[f(\eta,p),\omega(\eta,p),\theta(\eta,p),\phi(\eta,p)] \quad (14)$$

$$(1-p)L[\omega(\eta;p)-\omega_0(\eta)]=ph_2N_2[f(\eta,p),\omega(\eta,p),\theta(\eta,p),\phi(\eta,p)] \quad (15)$$

$$(1-p)L[\theta(\eta;p)-\theta_0(\eta)]=ph_3N_3[f(\eta,p),\omega(\eta,p),\theta(\eta,p),\phi(\eta,p)] \quad (16)$$

$$(1-p)L[\phi(\eta;p)-\phi_0(\eta)]=ph_4N_4[f(\eta,p),\omega(\eta,p),\theta(\eta,p),\phi(\eta,p)] \quad (17)$$

subject to the boundary conditions

$$\begin{array}{llll} f(0;p)=0, & f(1;p)=0, & \omega(0;p)=0, & \omega(1;p)=0 \\ \theta(0;p)=0, & \theta(1;p)=1, & \phi(0;p)=0, & \phi(1;p)=1 \end{array} \quad (18)$$

where $p\in[0,1]$ is the embedding parameter and the non-linear operators N_1, N_2, N_3 and N_4 are defined as:

$$N_1[f(\eta,p),\omega(\eta,p),\theta(\eta,p),\phi(\eta,p)]=\frac{1}{1-N}f''-Rf'+\frac{N}{1-N}\omega'+\frac{Gr_{\mathrm{T}}}{Re}\theta+\frac{Gr_{\mathrm{c}}}{Re}\phi-A \quad (19)$$

$$N_2[f(\eta,p),\omega(\eta,p),\theta(\eta,p),\phi(\eta,p)]=\frac{2-N}{m_{\mathrm{p}}^2}\omega''-aj\frac{1-N}{N}R\omega'-2\omega-f' \quad (20)$$

$$N_3[f(\eta,p),\omega(\eta,p),\theta(\eta,p),\phi(\eta,p)]$$

$$= \theta'' - RPr\theta' + \frac{Br}{1-N}\left[f'^2 + \frac{N(2-N)}{m_p^2}\omega'^2 + 2N(\omega^2 - \omega f')\right] + D_f Pr\phi'' \tag{21}$$

$$N_4[f(\eta, p), \omega(\eta, p), \theta(\eta, p), \phi(\eta, p)] = \frac{1}{Sc}\phi'' - R\phi' + S_r\theta'' \tag{22}$$

For $p = 0$ we have the initial guess approximations

$$f(\eta; 0) = f_0(\eta),\ \omega(\eta; 0) = \omega_0(\eta),\ \theta(\eta; 0) = \theta_0(\eta),\ \phi(\eta; 0) = \phi_0(\eta) \tag{23}$$

When $p = 1$, Eqs. (14)–(17) are same as (8)–(11) respectively, therefore at $p = 1$ we get the final solutions

$$f(\eta; 1) = f(\eta),\ \omega(\eta; 1) = \omega(\eta),\ \theta(\eta; 1) = \theta(\eta),\ \phi(\eta; 1) = \phi(\eta) \tag{24}$$

Hence the process of giving an increment to p from 0 to 1 is the process of $f(\eta; p)$ varying continuously from the initial guess $f_0(\eta)$ to the final solution $f(\eta)$ (similar for $\omega(\eta; p)$, $\theta(\eta; p)$ and $\phi(\eta; p)$). This kind of continuous variation is called deformation in topology so that we call system Eqs. (14)–(18), the zeroth-order deformation equation. Next, the mth-order deformation equations follow as

$$\begin{aligned} L[f_m(\eta) - \chi_m f_{m-1}(\eta)] &= h_1 R_m^f(\eta), \\ L[\omega_m(\eta) - \chi_m \omega_{m-1}(\eta)] &= h_2 R_m^\omega(\eta) \\ L[\theta_m(\eta) - \chi_m \theta_{m-1}(\eta)] &= h_3 R_m^\theta(\eta), \\ L[\phi_m(\eta) - \chi_m \phi_{m-1}(\eta)] &= h_4 R_m^\phi(\eta) \end{aligned} \tag{25}$$

with the boundary conditions

$$\begin{aligned} &f_m(0) = 0, \quad f_m(1) = 0, \quad \omega_m(0) = 0, \quad \omega_m(1) = 0 \\ &\theta_m(0) = 0, \quad \theta_m(1) = 0, \quad \phi_m(0) = 0, \quad \phi_m(1) = 0 \end{aligned} \tag{26}$$

where

$$R_m^f(\eta) = \frac{1}{1-N}f'' - Rf' + \frac{N}{1-N}\omega' + \frac{Gr_T}{Re}\theta + \frac{Gr_c}{Re}\phi - A(1-\chi_m) \tag{27}$$

$$R_m^\omega(\eta) = \frac{2-N}{m_p^2}\omega'' - aj\frac{1-N}{N}R\omega' - 2\omega - f' \tag{28}$$

$$R_m^\theta(\eta) = \theta'' - RPr\theta' + \frac{Br}{1-N}\left[\sum_{n=0}^{m-1} f'_{m-1-n}f'_n + \frac{N(2-N)}{m_p^2}\sum_{n=0}^{m-1}\omega'_{m-1-n}\omega'_n + 2N\left(\sum_{n=0}^{m-1}\omega_{m-1-n}\omega_n - \sum_{n=0}^{m-1}\omega_{m-1-n}f'_n\right)\right] + D_f Pr\phi'' \tag{29}$$

$$R_m^\phi(\eta) = \frac{1}{Sc}\phi'' - R\phi' + S_r\theta'' \tag{30}$$

for m being integer and

$$\chi_m = 0 \quad \text{for} \quad m \le 1 = 1 \quad \text{for} \quad m > 1 \tag{31}$$

The initial guess approximations $f_0(\eta)$, $\omega_0(\eta)$, $\theta_0(\eta)$ and $\phi_0(\eta)$, the linear operator L and the auxiliary parameters h_1, h_2, h_3 and h_4 are assumed to be selected such that Eqs. (14)–(18) have solution at each point $p \in [0, 1]$ and also with the help of Taylor's series and due to Eq. (23); $f(\eta; p)$, $\omega(\eta; p)$, $\theta(\eta; p)$ and $\phi(\eta; p)$ can be expressed as

$$\begin{aligned} f(\eta; p) &= f_0(\eta) + \sum_{m=1}^{\infty} f_m(\eta)p^m, \\ \omega(\eta; p) &= \omega_0(\eta) + \sum_{m=1}^{\infty} \omega_m(\eta)p^m, \\ \theta(\eta; p) &= \theta_0(\eta) + \sum_{m=1}^{\infty} \theta_m(\eta)p^m, \\ \phi(\eta; p) &= \phi_0(\eta) + \sum_{m=1}^{\infty} \phi_m(\eta)p^m, \end{aligned} \tag{32}$$

in which h_1, h_2, h_3 and h_4 are chosen in such a way that the series (32) are convergent at $p = 1$. Therefore we have from (24) that

$$\begin{aligned} f(\eta) &= f_0(\eta) + \sum_{m=1}^{\infty} f_m(\eta), \\ \omega(\eta) &= \omega_0(\eta) + \sum_{m=1}^{\infty} \omega_m(\eta), \\ \theta(\eta) &= \theta_0(\eta) + \sum_{m=1}^{\infty} \theta_m(\eta), \\ \phi(\eta) &= \phi_0(\eta) + \sum_{m=1}^{\infty} \phi_m(\eta), \end{aligned} \tag{33}$$

We presume that the initial guesses to f, ω, θ and ϕ the auxiliary linear operators L and the non-zero auxiliary parameters h_1, h_2, h_3 and h_4 are so properly selected that the deformation $f(\eta, p)$, $\omega(\eta, p)$, $\theta(\eta, p)$ and $\phi(\eta, p)$ are smooth enough and their mth-order derivatives with respect to p in Eq. (33) exist and are given respectively by $f_m(\eta) = \frac{1}{m!}\frac{\partial^m f(\eta;p)}{\partial p^m}\Big|_{p=0}$, $\omega_m(\eta) = \frac{1}{m!}\frac{\partial^m \omega(\eta;p)}{\partial p^m}\Big|_{p=0}$, $\theta_m(\eta) = \frac{1}{m!}\frac{\partial^m \theta(\eta;p)}{\partial p^m}\Big|_{p=0}$, $\phi_m(\eta) = \frac{1}{m!}\frac{\partial^m \phi(\eta;p)}{\partial p^m}\Big|_{p=0}$. It is clear that the convergence of Taylor series at $p = 1$ is a prior assumption, whose justification is provided Liao [17], so that the system in (33) holds true. The formulae in (33) provide us

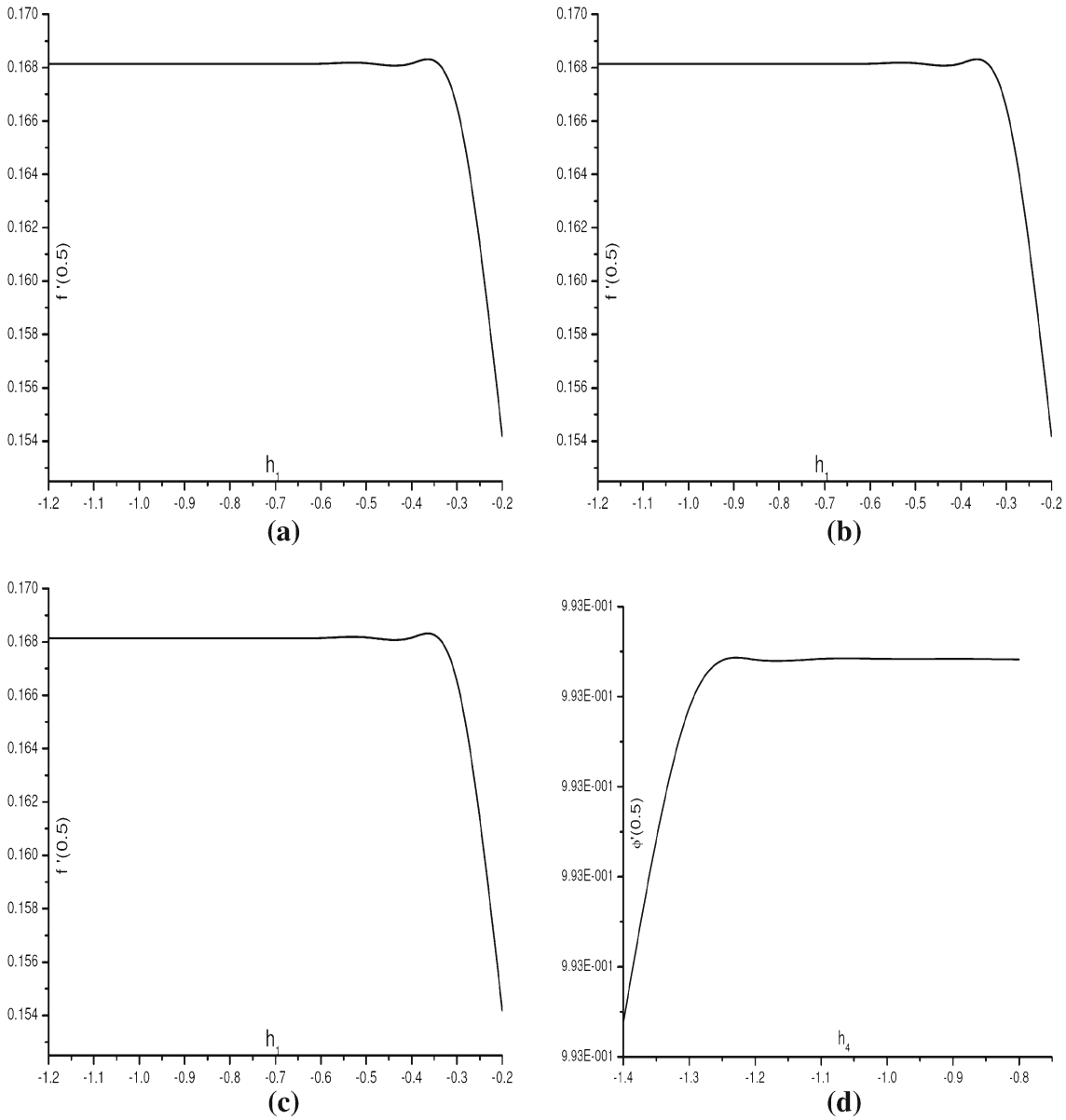

Fig. 1 The h curve of **a** $f(\eta)$, **b** $\omega(\eta)$, **c** $\theta(\eta)$, **d** $\phi(\eta)$, $D_{\mathrm{f}} = 2.0$ $S_{\mathrm{r}} = 0.03$; $N = 0.5$

with a direct relationship between the initial guesses and the exact solutions. All the effects of micropolar parameter, the heat and mass transfer, Soret and Dufour effects, velocity and microrotation can be studied from the exact formulas (33). Moreover, a special emphasis should be placed here because the mth-order deformation system (25) is a linear differential equation system with the auxiliary linear operators L whose fundamental solution is known.

4 Convergence of the HAM Solution

One of the chief aims of the HAM method is to produce solutions that will converge in a much larger region than the solutions obtained with traditional methods. Convergence of the solution series depends upon the choice of initial approximations, the auxiliary linear operators and the non-zero auxiliary parameters. By varying these parameters we can adjust the region in which the series is convergent and the rate at which the series converges. One of the major factors that influences the convergence of the solution series is the auxiliary parameters h_1, h_2, h_3 and h_4 as pointed by Liao [15]. For this purpose, the h-curves are plotted by choosing h_1, h_2, h_3 and h_4 in such a manner that the solutions (32) ensure convergence [17]. Here to see the admissible values of h_1, h_2, h_3 and h_4 the h-curves are plotted for 15th-order of approximation in Fig. 1 by taking the values of the parameters $Re = 1$, $R = 2$, $A = 1$, $Br = 1.0$, $Gr_{\mathrm{T}} = 0.2$, $Gr_{\mathrm{c}} = 2.0$,

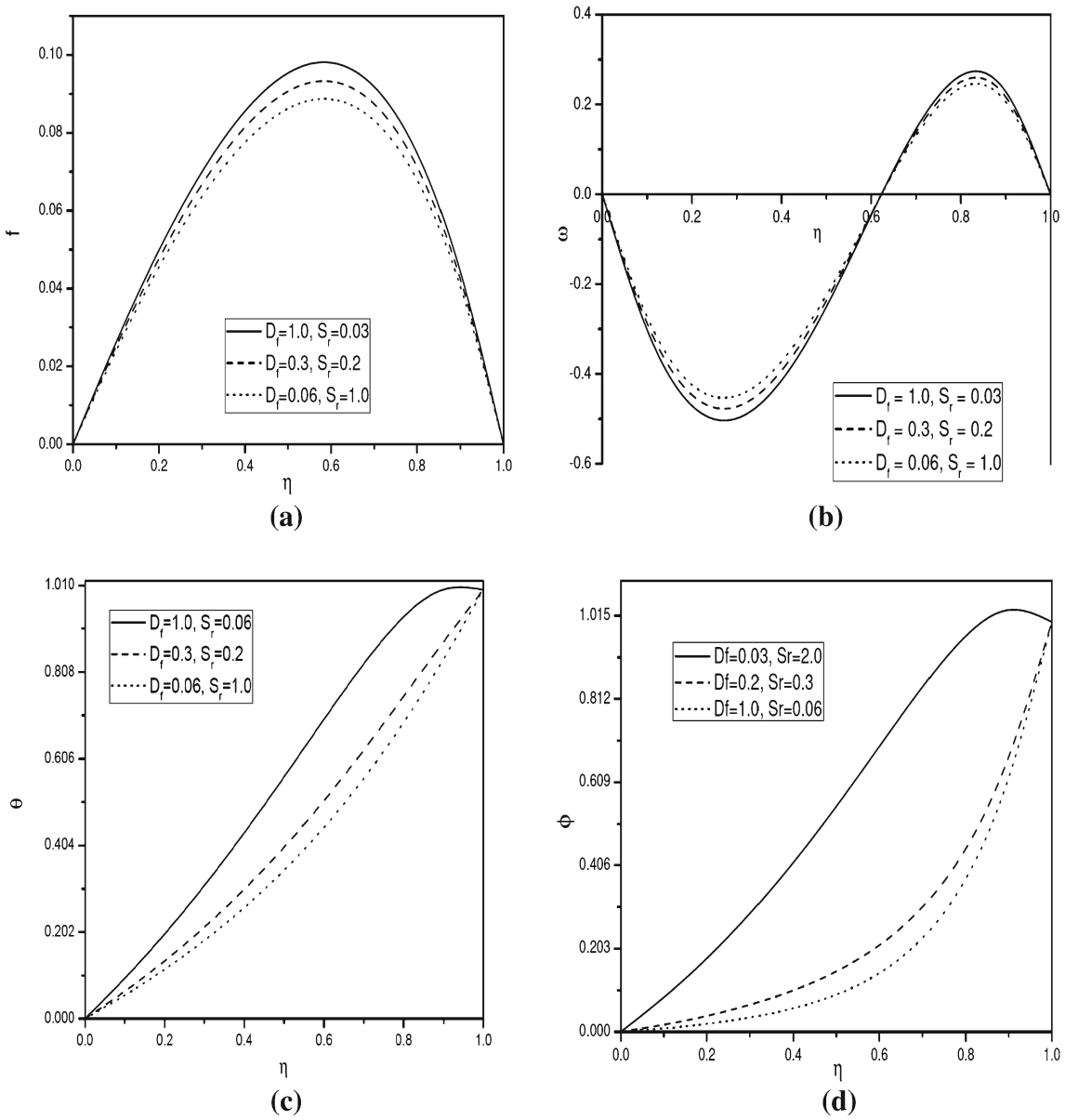

Fig. 2 Effect of Dufour and Soret numbers on **a** velocity (f), **b** microrotation, **c** temperature and **d** concentration for $N = 0.5$

$Pr = 0.71, N = 0.5, a_j = 0.001, m_p = 1.0, Sc = 0.2$, $D_f = 2.0$ and $S_r = 0.03$. It is noticed from Fig. 1a that the range for the admissible values of h_1 is $-1.2 < h_1 < -0.6$. From Fig. 1b, it is seen that the h-curve has a parallel line segment that corresponds to a region $-0.9 < h_2 < -0.6$. Figure 1c depicts the admissible values of h_3 as $-1.5 < h_3 < -1.0$. From Fig. 1d, it is observed that the range for the admissible values of h_4 is $-1.15 < h_4 < -0.8$. A wide valid zone is evident in these figures ensuring convergence of the series.

To choose optimal value of auxiliary parameter, the average residual errors (see Reference [17] for more details) are calculated at different order of approximations (m). Also, for optimality of the convergence control parameters, relative errors [18] are calculated for different values of h in the convergence region. It is found the series given by (32) converge in the whole region of η when $h_1 = -0.9$, $h_2 = -0.7$, $h_3 = -1.2, h_4 = -1.0$.

5 Results and Discussion

In order to investigate the effects of the different parameters, the numerical values of velocity (f), microrotation (ω), temperature (θ) and the species concentrations (ϕ) are computed by taking $Pr = 0.71$, $Sc = 2.0$, $A = 1$, $Br = 1.0$, $Gr_T = 0.2$, $Gr_c = 2.0$, $a_j = 0.001$, $m = 1$, $R = 2.0$ and $Re = 1$. The values of Soret number S_r and Dufour number D_f are chosen in such a way that their product is constant

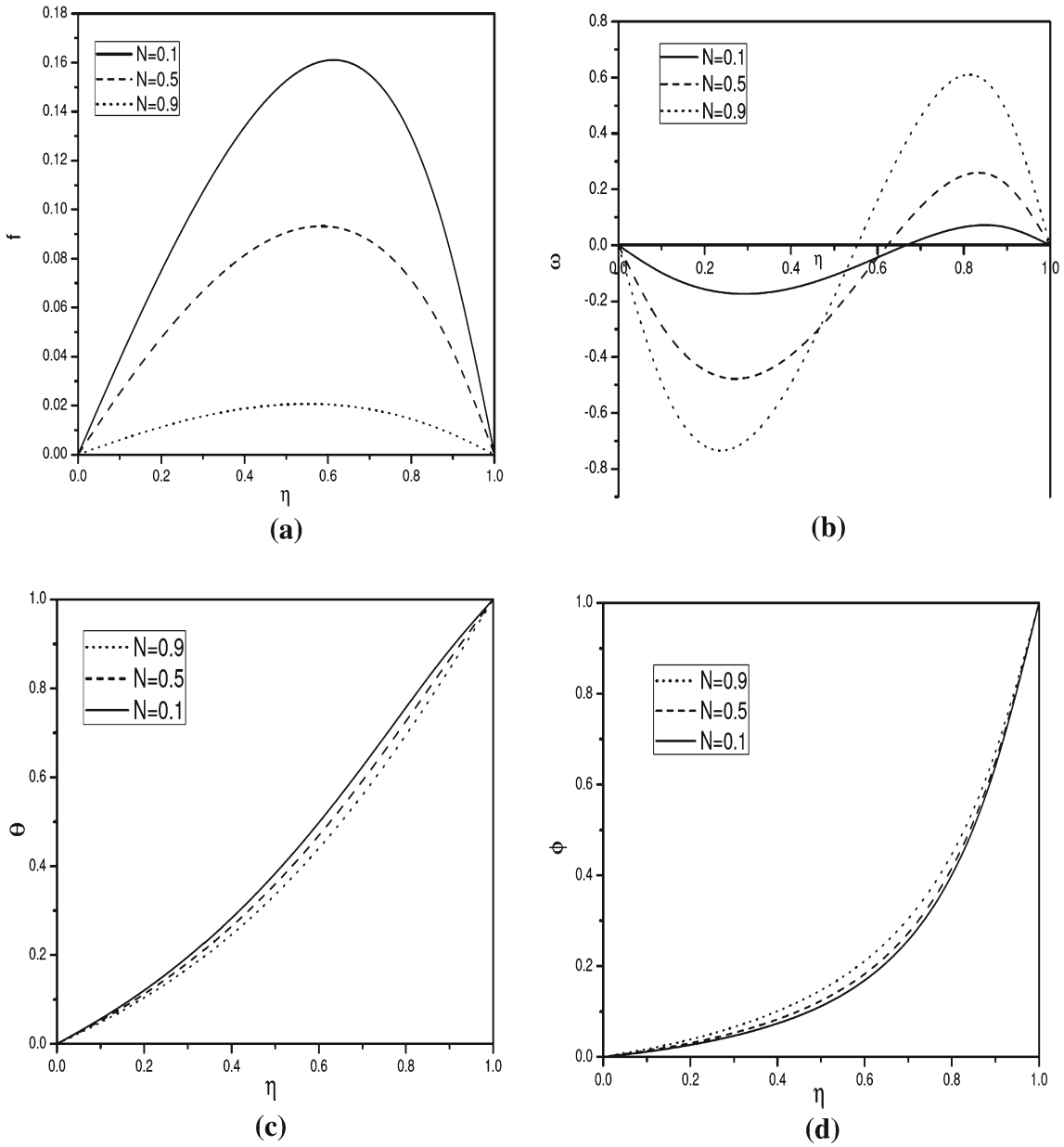

Fig. 3 Effect of coupling numbers on **a** velocity (f), **b** microrotation, **c** temperature and **d** concentration for $D_f = 0.03$, $S_r = 2$

according to their definition provided that the mean temperature T_m is kept constant [8]. These values are used throughout the computations, unless otherwise indicated.

Figure 2 displays the effects of Soret number S_r and Dufour number D_f on non-dimensional velocity, microrotation, temperature and concentration for $N = 0.5$ and $R = 2$. It is observed from Fig. 2a that the velocity of the fluid decreases with the decrease of Dufour number (or increase of Soret number). Figure 2b demonstrates that the increase (decrease) in the value of Dufour (Soret) number increases the microrotation in magnitude. The values of microrotation are initially negative near the lower plate and positive near the upper plate, showing a reverse rotation near the two boundaries. The reason is that the microrotation field in this region is dominated by a small number of particles spins that are generated by collisions with the boundary. It is noticed from Fig. 2c that the temperature of the fluid increases with the increase in the value of the Dufour number D_f. It is clear from Fig. 2d that the non-dimensional concentration of the fluid decreases with the increase of Dufour number D_f (or decrease of Soret number). The Dufour number denotes the contribution of the concentration gradients to the thermal en-

Table 1 Effects of skin friction, heat and mass transfer coefficients for varying values of coupling, Soret, Dufour and suction/injuction Reynolds numbers

N	D_f	S_r	R	Lower plate			Upper plate		
				$f'(0)$	$\theta'(0)$	$\phi'(0)$	$f'(1)$	$\theta'(1)$	$\phi'(1)$
0.1	0.03	2.0	2.0	0.50696	0.77758	0.89527	−1.34676	1.17454	1.13649
0.3	0.03	2.0	2.0	0.43407	0.76516	0.899821	−1.0088	1.22429	1.11617
0.5	0.03	2.0	2.0	0.3399	0.749861	0.90549	−0.69148	1.27289	1.09629
0.7	0.03	2.0	2.0	0.22239	0.73134	0.91249	−0.39698	1.31898	1.07742
0.9	0.03	2.0	2.0	0.11802	0.72110	0.91595	−0.19154	1.33145	1.07432
0.4	0.03	2.0	3.0	0.33112	0.74892	0.81875	−0.88641	1.24766	1.21926
0.4	0.03	2.0	2.0	0.38983	0.75787	0.90251	−0.84740	1.24882	1.10614
0.4	0.03	2.0	1.0	0.45596	0.76770	0.99244	−0.801144	1.2524	0.99856
0.4	0.03	2.0	−1.0	0.60408	0.78779	1.19202	−0.69305	1.26719	0.80026
0.4	0.03	2.0	−2.0	0.68153	0.79669	1.30229	−0.63563	1.27776	0.70986
0.4	0.03	2.0	−3.0	0.75802	0.80402	1.41985	−0.57908	1.28962	0.62560
0.4	0.03	2.0	2.0	0.38983	0.75787	0.90251	−0.84740	1.24882	1.10614
0.4	0.06	1.0	2.0	0.38561	0.76115	0.85731	−0.84009	1.24474	1.16059
0.4	0.12	0.5	2.0	0.38355	0.77025	0.83446	−0.83652	1.23185	1.18831
0.4	2.0	0.03	2.0	0.38126	1.08063	0.81285	−0.83777	0.78031	1.21466

ergy flux in the flow. It can be seen that an increase in the Dufour number causes a rise in the velocity and temperature and a drop in the concentration.

The effect of coupling number on velocity, microrotation, temperature and concentration is presented in Fig. 3. The coupling number N characterizes the coupling of linear and rotational motion arising from the micromotion of the fluid molecules. Hence N signifies the coupling between the Newtonian (μ) and rotational viscosities (κ) and hence $0 \leq N < 1$. With a large value of N the effect of microstructure becomes significant, whereas with a small value of N the individuality of the substructure is much less pronounced. As $\kappa \to 0$ i.e. $N \to 0$, the micropolarity is lost and the fluid behaves as non-polar fluid. Hence, $N \to 0$ corresponds to viscous fluid. It is observed from Fig. 3a that the velocity decreases with the increase of coupling number N. The maximum of velocity decreases in amplitude with an increase of N. The velocity in case of micropolar fluid is less than that in the viscous fluid case. It is seen from Fig. 3b that the microrotation component decreases near the lower plate and increases near the upper plate with increasing coupling number N. The microrotation tends to zero as $N \to 0$. It is noticed from Fig.3c that the non-dimensional fluid temperature decreases with increasing values of coupling number. Hence micropolar effects behave as a coolant and are thus effective in reducing the cooling rate and help in producing the desired temperature. It is clear from Fig. 3d that the non-dimensional fluid concentration increases with increasing values of N.

The skin friction is defined as $C_f = \dfrac{2\tau_w}{\rho U_0^2}$, where $\tau_w = (\mu + \kappa)\dfrac{\partial u}{\partial y} + \kappa\Gamma$ is the wall shear stress. Hence the skin friction factors at the upper and lower plates, respectively, are given by:

$$C_{f_1} Re = \left(\frac{2}{1-N}\right) f'(1), \quad C_{f_2} Re \left(\frac{2}{1-N}\right) f'(0) \tag{34}$$

The non-dimensional rate of heat-transfer, called the Nusselt number, is defined as $Nu = \left(\dfrac{\partial T}{\partial n}\right)_w / (T_2 - T_1)$, where $\left(\dfrac{\partial T}{\partial n}\right)_w$ the temperature gradient in normal direction to the plates. Similarly the non-dimensional rate of mass transfer, called the Sherwood number, is defined as: $Sh = \left(\dfrac{\partial C}{\partial n}\right)_w / (C_2 - C_1)$, where $\left(\dfrac{\partial C}{\partial n}\right)_w$ denote the concentration gradient in normal direction to the plates. The heat and mass transfer rates on the two plates are given by:

$$Nu_1 = -\theta'(0), \quad Nu_2 = -\theta'(1) \quad \text{and}$$
$$Sh_1 = -\phi'(0), \quad Sh_2 = -\phi'(1) \tag{35}$$

The variations of $f'(0), f'(1), \theta'(0), \theta'(1), \phi'(0)$ and $\phi'(1)$ which are proportional to the local skin friction coefficient, rate of heat and mass transfers at the lower and upper plates are shown in Table 1 for different values of the cou-

pling number, suction parameter Dufour and Soret number. From this table it is observed that the value of skin friction at both the plates is decreasing with the increasing values of coupling number. The heat transfer rate decreases with the increasing values of coupling number at the lower plate whereas the reverse effect is observed at the upper plate. Decrease in Soret number decreases the skin friction and mass transfer but increases the heat transfer at the lower plate. From these data it is seen that micropolar fluids reduce skin friction as compared to the Newtonian fluid; this may be beneficial in flow, temperature and concentration control of polymer processing.

6 Conclusions

A mathematical model has been presented for incompressible heat and mass transfer of a micropolar fluid between porous parallel plates. The model has been transformed and rendered into dimensionless form and solved using the approximate analytical series solutions HAM. It is found that the velocity decreases with an increase in micropolar parameter N. The micropolar effects behave as a coolant and are thus effective in reducing the cooling rate and help in producing desired temperature. It is hoped that the present investigation of the study of physics of flow can contribute its part for many scientific and engineering applications and for studying more complex geometry problems.

References

1. Ericksen, J.C.: Anisotropic fluids. Arch. Ration. Mech. Anal. **4**, 231–237 (1960)
2. Ericksen, J.C.: Transversely isotropic fluids. Colloid Polym. Sci. **173**, 117–122 (1960)
3. Hoyt, J.W.; Fabula, A.G.: US Naval Ordinance Test Station Report (1964)
4. Eringen, A.C.: Theory of micropolar fluids. J. Math. Mech. **16**, 1–18 (1966)
5. Lukaszewicz, G.: Micropolar Fluids—Theory and Applications. Birkhauser, Basel (1999)
6. Eckert, E.R.G.; Drake, R.M.: Analysis of Heat and Mass Transfer. McGraw-Hill, NewYork (1972)
7. Dursunkaya, Z.; Worek, W.M.: Diffusion-thermo and thermal-diffusion effects in transient and steady natural convection from vertical surface. Int. J. Heat Mass Transf. **35**, 2060–2065 (1992)
8. Kafoussias, N.G.; Williams, N.G.: Thermal-diffusion and diffusion-thermo effects on mixed free-forced convective and mass transfer boundary layer flow with temperature dependent viscosity. Int. J. Eng. Sci. **33**, 1369–1384 (1995)
9. Awad, F.; Sibanda, P.: Dufour and Soret effects on heat and mass transfer in a micropolar fluid in a horizontal channel. WSEAS Trans. Heat Mass Transf. **5**(3), 165–177 (2010)
10. Jha, B.K.; Ajibade, A.O.: Free convection heat and mass transfer flow in a vertical channel with the Dufour effect. Proc. ImechE Part E J. Process Mech. Eng. **224**, 91–101 (2011)
11. Olanrewaju, P.O.; Makinde, O.D.: Effects of thermal diffusion and diffusion thermo on chemically reacting MHD boundary layer flow of heat and mass transfer past a moving vertical plate with suction/injection. Arab. J. Sci. Eng. **36**(8), 1607–1619 (2011)
12. Srinivasacharya, D.; Kaladhar, K.: Analytical solution for chemically reacting free convective couple stress fluid in an annulus with Soret and Dufour effects. Int. Rev. Mech. Eng. **5**(5), 823–833 (2011)
13. Elaiw, A.M.; Ibrahim, F.S.; Bakr, A.A.; Salama, A.A.: Effect of variable viscosity on vortex instability of mixed convection boundary layer flow adjacent to a non-isothermal horizontal surface in a porous medium. Arab. J. Sci. Eng. **36**(8), 1517–1528 (2011)
14. Mokheimer, E.M.A.: Buoyancy effects on entropy generation in the entrance region of isothermal/adiabatic vertical channel. Arab. J. Sci. Eng. **37**(6), 1681–1700 (2012)
15. Liao, S.J.: Beyond Perturbation. Introduction to Homotopy Analysis Method. Chapman and Hall/CRC Press, Boca Raton (2003)
16. Liao, S.J.: On the homotopy analysis method for nonlinear problems. Appl. Math. Comput. **147**(2), 499–513 (2004)
17. Liao, S.J.: An optimal homotopy-analysis approach for strongly nonlinear differential equations. Commun. Nonlinear Sci. Numer. Simul. **15**, 2003–2016 (2010)
18. Rashidi, M.M.; Mohimanian Pour, S.A.; Abbasbandy, S.: Analytic approximate solutions for heat transfer of a micropolar fluid through a porous medium with radiation. Commun. Nonlinear Sci. Numer. Simul. **16**, 1874–1889 (2011)